

# A Black Hole Mass-Variability Time Scale Correlation at Submillimeter Wavelengths

Geoffrey C. Bower,<sup>1</sup> Jason Dexter,<sup>2</sup> Sera Markoff,<sup>3</sup> Mark A. Gurwell,<sup>4</sup> Ramprasad Rao,<sup>1</sup>  
Ian McHardy<sup>5</sup>

## ABSTRACT

We analyze the light curves of 413 radio sources at submillimeter wavelengths using data from the Submillimeter Array calibrator database. The database includes more than 20,000 observations at 1.3 and 0.8 mm that span 13 years. We model the light curves as a damped random walk and determine a characteristic time scale  $\tau$  at which the variability amplitude saturates. For the vast majority of sources, primarily blazars and BL Lac objects, we find only lower limits on  $\tau$ . For two nearby low luminosity active galactic nuclei, M81 and M87, however, we measure  $\tau = 1.6_{-0.9}^{+3.0}$  days and  $\tau = 45_{-24}^{+61}$  days, respectively ( $2\sigma$  errors). Including the previously measured  $\tau = 0.33 \pm 0.16$  days for Sgr A\*, we show an approximately linear correlation between  $\tau$  and black hole mass for these nearby LLAGN. Other LLAGN with spectra that peak in the submm are expected to follow this correlation. These characteristic time scales are comparable to the minimum time scale for emission processes close to an event horizon, and suggest that the underlying physics may be independent of black hole mass, accretion rate, and jet luminosity.

*Subject headings:* black hole physics, accretion, galaxies: jets, galaxies: active, Galaxy: center

---

<sup>1</sup>Academia Sinica Institute of Astronomy and Astrophysics, 645 N. A'ohoku Place, Hilo, HI 96720, USA; gbower@asiaa.sinica.edu.tw

<sup>2</sup>Max Planck Institute for Extraterrestrial Physics, Giessenbachstr. 1, 85748 Garching, Germany

<sup>3</sup>Anton Pannekoek Institute for Astronomy, University of Amsterdam, Science Park 904, 1098 XH Amsterdam, The Netherlands

<sup>4</sup>Harvard-Smithsonian Center for Astrophysics, 60 Garden Street, Cambridge, MA 02138, USA

<sup>5</sup>Department of Physics and Astronomy, The University, Southampton SO17 1BJ, UK

## 1. Introduction

In recent years there has been much work focused on understanding black hole accretion and its similarities across the mass scale, from stellar mass black holes in X-ray binaries (BHBs) to active galactic nuclei (AGN). Long term variability studies have found evidence for a mass-dependence in timing features that holds from BHB to AGN (McHardy et al. 2006; Kelly et al. 2009; MacLeod et al. 2010). A linear correlation can be understood if the emission originates in a region that is the same size for all systems in units of Schwarzschild radii, where  $R_S = 2GM/c^2$ . However, the timescale is also inversely proportional to the Eddington accretion fraction, suggesting that the pertinent size of the emission zone is also regulated by the total system power. Similarly, studies of broadband spectra have found a strong correlation between radio and X-ray luminosity and black hole mass (the “Fundamental Plane of Black Hole Accretion”, or FP, see e.g., Merloni et al. 2003; Falcke et al. 2004; Plotkin et al. 2012), that have confirmed earlier theoretical frameworks (Blandford & Konigl 1979; Falcke & Biermann 1995) that synchrotron spectral features scale predictably with black hole mass and accretion power. Combining these concepts, observations at a fixed frequency of black holes of the same mass with different accretion power should not yield similar timescales, because the frequency “selects” out different sized emission regions in both cases.

The sub-millimeter (submm) band seems to be selecting out regions of event-horizon scale in two sources of drastically different mass and accretion rate: Sgr A\* and M87 (Doeleman et al. 2008, 2012a,b). Both sources belong to the class of nearby, low-luminosity AGN (LLAGN; Ho 1999) that fall on the FP.

Variability provides an independent test of the size scales. Dexter et al. (2014) used submm light curves to demonstrate that Sgr A\* follows a damped-random walk (DRW) variability pattern, with a characteristic time scale  $\tau = 8_{-4}^{+3}$  h at 230 GHz at 95 per cent confidence, with consistent results at higher frequencies. This time scale is an order of magnitude larger than the period of the last stable orbit for a non-rotating black hole, which is most easily understood as resulting from accretion processes on a scale of a few to  $\sim 10R_S$ .

We present a variability study of AGN in the submm, including the LLAGN M81 and M87 as well as the 411 other radio sources included in the SMA Calibrator database, which span more than a decade in duration (§2). This sample was previously analyzed by Strom et al. (2010), but with a much smaller number of objects and total span. The full sample of light curves are well described by a noise process, which we model with a damped random walk in order to quantitatively measure characteristic variability time scales (§3). We show that the LLAGN follow a correlation between black hole mass and time scale, while the higher luminosity AGN have much longer characteristic time scales with no clear black hole

mass dependence.

## 2. Data Sample

The SMA calibrator database (Gurwell et al. 2007) includes observations of 412 sources from June 2002 to January 2015. A total of 23254 flux densities are recorded with 19111 of those flux densities obtained in the 1.3mm band. 410 light curves have  $> 10$  flux densities, 141 light curves have  $> 30$  flux densities, and 48 light curves have  $> 100$  flux densities. Observations were obtained at frequencies from 200 to 406 GHz with 70% obtained between 220 and 235 GHz. 165 observations (147 at 1.3mm) of M87 are included in the calibrator database spanning from January 2003 to January 2015. Data reduction of sources followed standard SMA techniques that set flux densities on absolute flux density scales determined by solar system objects with typical accuracy of 5 to 10%.

Sources are selected for the SMA calibrator database on the basis of their suitability as phase reference sources for mm/submm interferometric observations, primarily reflected in their compact size, bright radio flux density, and declination above  $-50^\circ$ . Flux densities in the data base range from 26 mJy to 52 Jy with a median value of 1.2 Jy. 336 sources are matched to flat spectrum radio sources in the CRATES catalog (Healey et al. 2007). Non-matches to CRATES include steep spectrum calibrators such as 3C 286 and sources in the Galactic plane such as J1700-261 that may have been missed by the single dish surveys that form the basis of CRATES. The CRATES sample includes primarily blazars and BL Lac sources; 289 of the sources are found in the CGRABS catalog of  $\gamma$ -ray blazar candidates (Healey et al. 2008).

We also included SMA monitoring observations of M81 in our analysis, which has been the target of a significant campaign (McHardy et al. 2015). This campaign included 86 observations between September 2009 and March 2012, of which 42 observations were obtained at frequencies higher than 300 GHz. We also include PdBI observations of M81 obtained in 2005 at 1.3 mm with a time resolution of  $\sim 1$  hour (Schödel et al. 2007).

## 3. Time Scale Analysis

The light curve for M87 is shown in Figure 1. The light curve for M81 is shown in McHardy et al. (2015) and shares similar characteristics of short-term variability and long-term stability. These properties are visible in the structure functions (Fig.2), defined for a

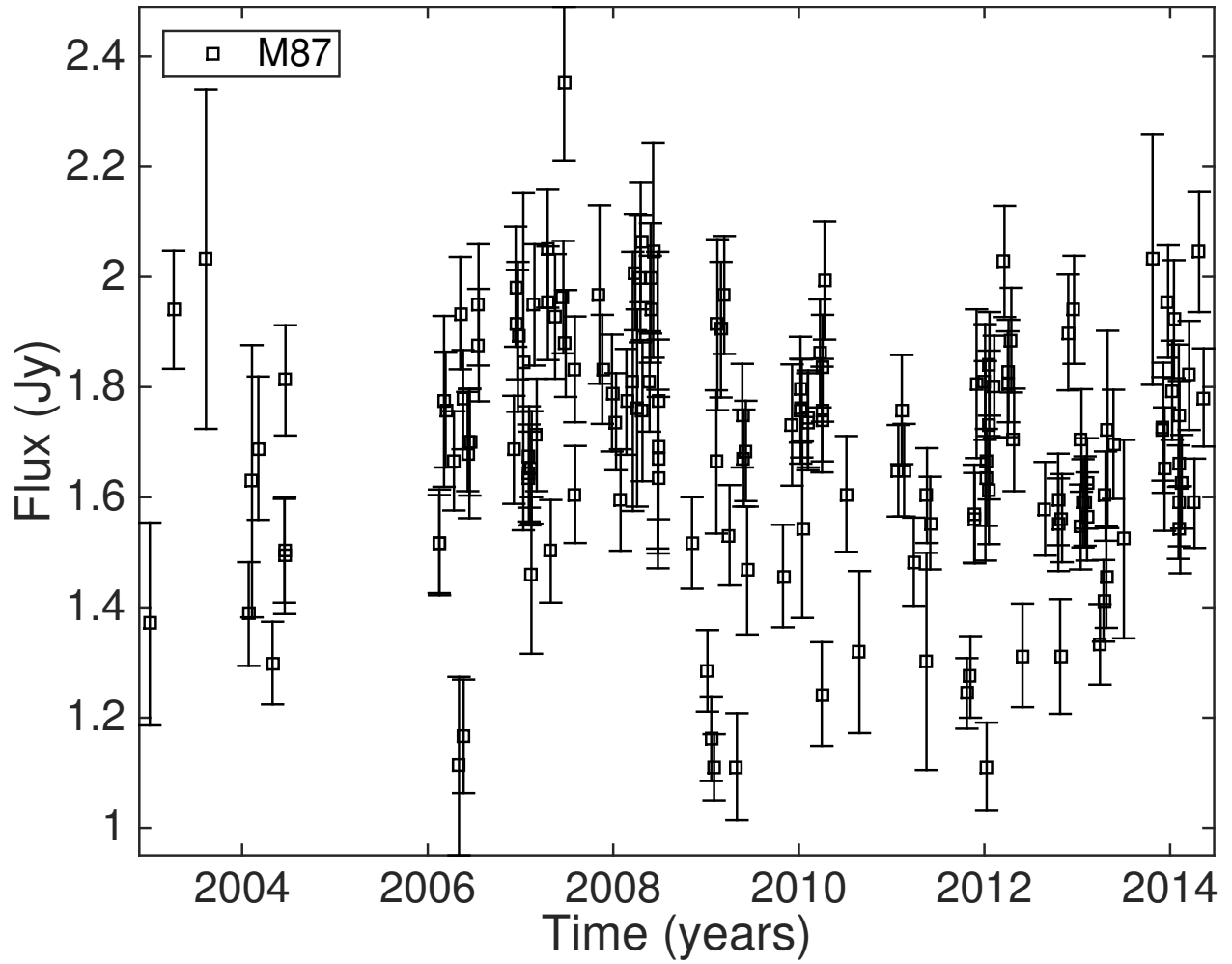


Fig. 1.— Light curve for M87 at 1.3 mm from the SMA. The light curves show the characteristic of short-term variability coupled with long-term stability that is the signature of the damped random walk.

light curve  $s(t)$  with  $N$  data points as

$$S^2(\Delta t) = \frac{1}{N} \sum (s(t) - s(t + \Delta t))^2. \quad (1)$$

Both structure functions show increases in activity on short time scales followed by a plateau, similar to those of Sgr A\* (Dexter et al. 2014) but markedly different than those of typical calibrators in the database. For instance, the structure functions for 3C 84 and 279 rise smoothly without any apparent saturation time scale for  $\Delta t < 10\text{yr}$ . Structure functions are a useful guide for qualitative comparison; however, they functions are unreliable for quantitative analysis (Emmanoulopoulos et al. 2010). They can show artifacts from aliasing (e.g. peaks at  $\sim 180$  days associated with the annual cycle), as well as spurious saturation time scales even with regularly sampled data. Fitting of structure functions for saturation time scales is also challenging since their values and errors at different time scales are correlated.

### 3.1. Damped random walk model

In order to quantitatively measure characteristic time scales, we model the entire set of submm light curves as the result of a stochastic damped random walk (DRW) process. The DRW is a simple 3-parameter model (mean, standard deviation of long-timescales, and transition time) that is well-suited to parametrize the most important properties of noise light curves (Kelly et al. 2009). The DRW consists of red-noise on time scales less than  $\tau$  and white-noise on longer time scales. The resultant structure function for the DRW is

$$S^2(\tau) = S_\infty^2 (1 - e^{-|\Delta t|/\tau}), \quad (2)$$

where  $S_\infty^2$  is the power in the light curve on long time scales  $\Delta t \gg \tau$ . The characteristic time scale  $\tau$  determines the de-correlation time on which the variability transitions from red noise on short timescales to white noise on long time scales. This model has been shown to successfully describe the optical light curves of quasars (Kelly et al. 2009; MacLeod et al. 2010), as well as the submm light curve of Sgr A\* (Dexter et al. 2014).

We convert the likelihood of the observed light curves arising from a given set of DRW parameters into the posterior probability of the set of model parameters using a Bayesian approach. Kelly et al. (2009) and Dexter et al. (2014) used a Metropolis-Hastings algorithm to sample the likelihood over the model parameter space. We use this approach to measure the model parameters in cases where the upper limit to  $\tau$  is smaller than the light curve duration  $T$ . However, this is not the case for the vast majority of the SMA calibrator light curves. When no upper limit can be found, the Metropolis-Hastings algorithm fails, as it preferentially samples the long tail of the probability distribution rather than its peak.

To avoid this issue, we sample the probability distribution over a regular  $64^3$  grid in the parameters with uniform priors for the mean ( $\mu$ ), standard deviation ( $\log \sigma$ ), and  $\log \tau$ . Since for the vast majority of sources we are interested in lower limits on  $\tau$ , we choose the parameter ranges to ensure that the lower end and peak of the probability distribution are well captured, at the expense of the long tails to large  $\tau$  (much longer than the duration of the light curve). From the probability distributions in  $\tau$ , we consider good limits to be cases where  $\tau > \Delta t$  and  $\tau < T$  at 99.7% confidence, where  $\Delta t$  is the minimum separation between two measured points in the light curve and  $T$  is the total light curve duration. In all cases we report  $2\sigma$  limits because of the non-Gaussian nature of the distributions that can include long tails.

Although less efficient than Monte Carlo, this direct grid method recovers consistent parameter estimates for the M81 and M87 light curves. If the true light curve is not described by the DRW, as seen in Kepler quasar light curves (Kasliwal et al. 2015), the resulting  $\tau$  estimate will be biased. For light curves that can successfully be fit by the model ( $\chi_\nu^2 \sim 1$ ), such as the SMA data used here, the bias leads to  $< 1\sigma$  changes in our estimates of  $\tau$ .

### 3.2. Results

We use the DRW model to infer  $\tau$  values from the full set of 664 230 and 345 GHz light curves from the 413 sources. A histogram of the resulting 95% confidence lower and upper limits on  $\tau$  is shown in Figure 3. In total, we find 276 light curves with lower limits (40%) and 16 with upper limits (2%). The histograms are further broken down by sources with  $> 30$  data points and those with available black hole mass estimates in the literature (see below). For the measured lower limits, the sub-samples are consistent with the full sample. Many of the measured upper limits are false positives in light curves with few data points caused by not sampling a large enough range in  $\tau$ . After those are removed, 5 detections of upper limits remain, all of which have  $\chi_\nu^2$  close to unity, similar to Sgr A\*. In Table 1, we summarize the detections. The light curve residuals after model subtraction are normally distributed for M81 and M87, as expected for an accurate model, and similar to what was seen for Sgr A\* (Dexter et al. 2014).

The results of this time scale analysis are in stark contrast for the available LLAGN light curves (Sgr A\*, M81, M87) and those of ordinary AGN / blazars (the vast majority of the light curves). For the LLAGN, 3/3 sources have well measured values of  $\tau$ . For the rest of the sources, 1% (4/664) have reliable measurements of  $\tau$ . It is therefore potentially possible to select LLAGN based on submm properties alone, with a low false positive rate and a high detection efficiency for well sampled light curves. There is no systematic difference in the

number or cadence of measured flux densities that can explain this result: it is related to an intrinsic difference in the submm variability properties of the different source classes.

### 3.3. Black Hole Mass Estimates

We compiled black hole masses from the literature. The three nearby LLAGN have the most accurately determined masses, often from multiple dynamical methods. Sgr A\* has a mass of  $4.4 \times 10^6 M_\odot$  (Genzel et al. 2010). M87 has a mass of  $3.5_{-0.7}^{+0.9} \times 10^9 M_\odot$  from gas dynamic measurements (Walsh et al. 2013) and a mass of  $6.6 \pm 0.4 \times 10^9 M_\odot$  from stellar dynamic measurements (Gebhardt et al. 2011). Following Kormendy & Ho (2013), we adopt a value of  $6.2 \times 10^9 M_\odot$ . Similarly for M81, stellar and gas dynamical measurements exist (Bower et al. 2000; Devereux et al. 2003) and we follow Kormendy & Ho (2013) to adopt a value of  $6.5 \times 10^7 M_\odot$ .

For the remainder of the sample, we rely on published black hole mass estimates from various techniques. These include broad line region spectroscopy (Woo & Urry 2002; Kelly & Bechtold 2007; Shen et al. 2008, 2011; Pâris et al. 2014), black hole mass-bulge luminosity correlation (Woo & Urry 2002), and the FP between radio-X-ray luminosity (Merloni et al. 2003; Plotkin et al. 2012). For the case of Pâris et al. (2014), which does not provide mass estimates, we use their measurements of the Mg II transition and the methodology of Shen et al. (2011) to estimate masses. FP estimates of the black hole mass are derived using ROSAT 0.2 - 2.0 keV X-ray fluxes and the 1.3mm flux density that is debeamed assuming a Doppler boosting factor of 7. We identify 194 black hole mass measurements for 148 sources. For sources with multiple mass estimates, we rely on the most recent published estimate. The accuracy of the mass estimates range from 0.16 dex for Mg II transitions to  $> 0.4$  dex for continuum luminosity (Shen et al. 2011).

## 4. Discussion

The  $\tau$ - $M_{\text{BH}}$  relationship for the sub-sample of SMA calibrator sources with black hole mass estimates is shown in Figure 4. The difference in submm variability properties between regular and low-luminosity AGN is immediately apparent: the vast majority of AGN only yield lower limits on  $\tau$ , while the LLAGN have measured time scales that lie well below many of these at comparable black hole mass.

On the other hand, the measured  $\tau$  values for the 3 LLAGN with good measurements of  $\tau$  do show a significant trend of increasing  $\tau$  with increasing black hole mass. Formally, the

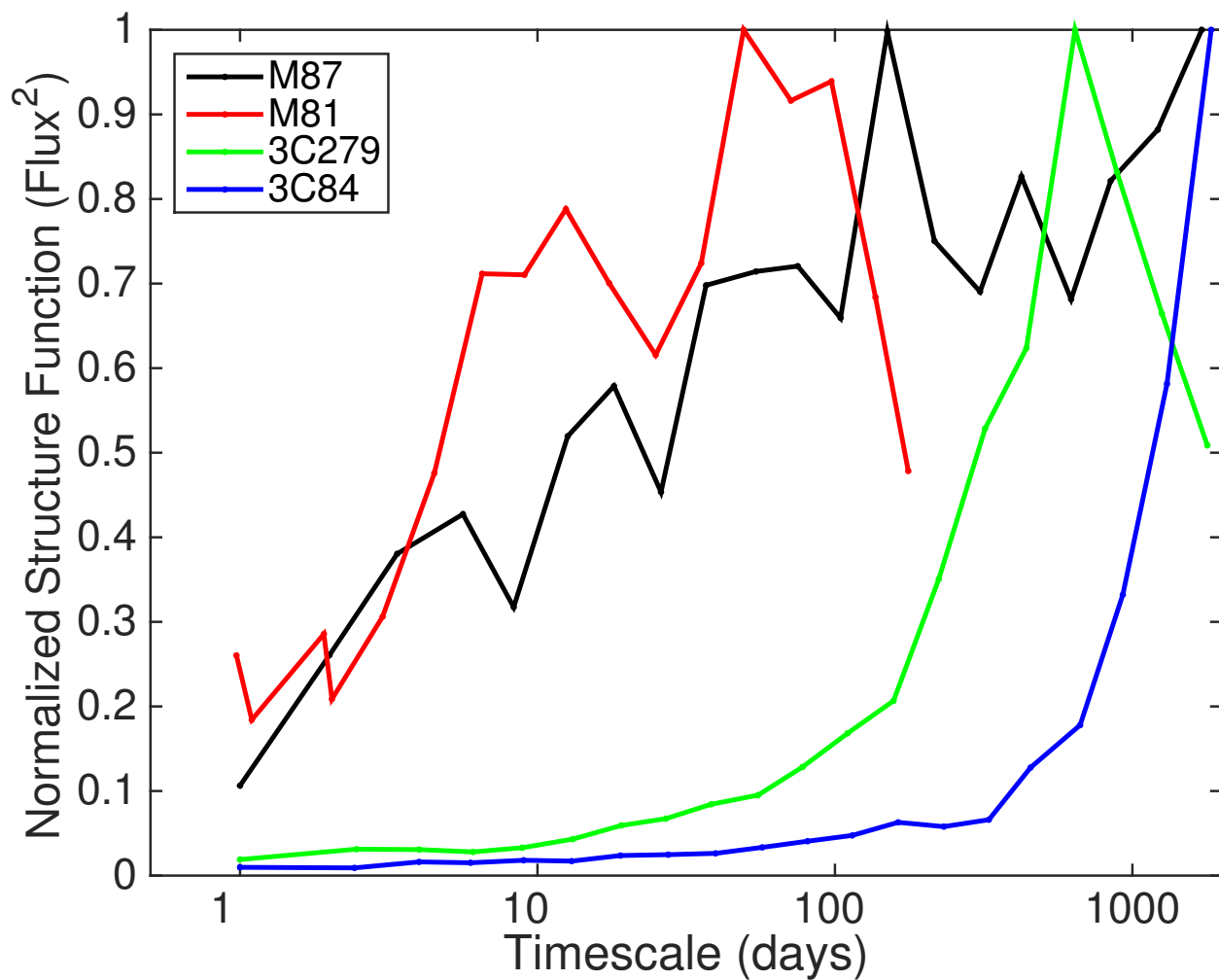


Fig. 2.— Structure functions for M87, M81, 3C 279, and 3C 84 from 1.3 mm SMA data. The structure function suggests that M87 and M81 have different variability characteristics from the two high power radio sources. Quantitative analysis with the DRW model confirms the differences.



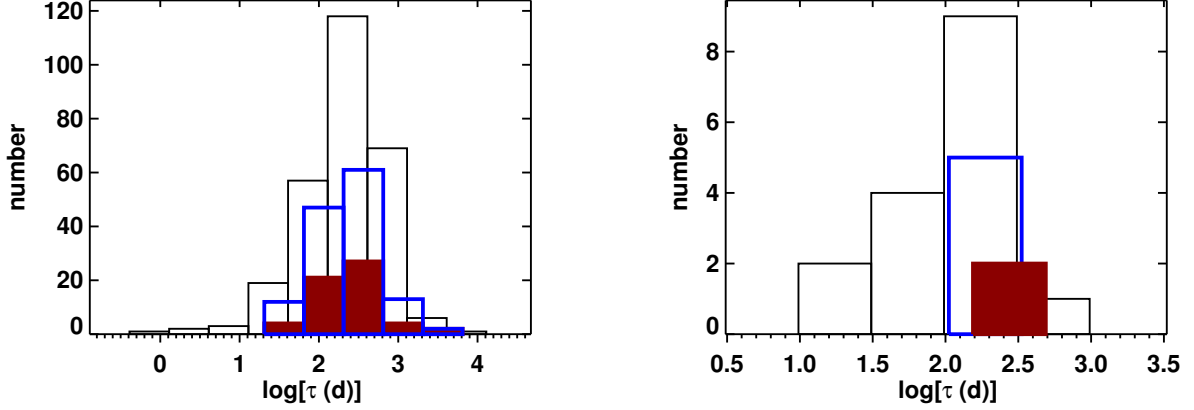


Fig. 3.— Histogram of  $\tau$  lower (left) and upper (right) limits for entire sample (black), those with  $n > 30$  (blue), and those with  $n > 30$  and black hole mass measurements (red). Constraints with  $n < 30$  are used to avoid false positives. Those with black hole masses are representative of overall distribution.

Table 1. Characteristic Time Scales for Submm Variability

Source	$\tau$ (days)	$\tau_{\text{low}}$ (days)	$\tau_{\text{high}}$ (days)	$\chi^2_\nu$	$M_{BH}$ ( $M_\odot$ )	Source
0433+053	106	63	299	0.88	$2.6 \times 10^7$	Woo & Urry (2002)
0721+713	75	56	155	0.83	$5.2 \times 10^6$	Fundamental Plane
1104+382	40	16	154	0.81	$1.9 \times 10^8$	Woo & Urry (2002)
1751+096	106	50	331	1.04	$2.2 \times 10^7$	Fundamental Plane
M87	45	21	106	0.87	$6.2 \times 10^9$	Kormendy & Ho (2013)
M81	1.6	0.7	4.6	1.14	$6.5 \times 10^7$	Cappellari et al. (2009)
Sgr A* <sup>1</sup>	0.33	0.17	0.5	1.05	$4.4 \times 10^6$	Genzel et al. (2010)

<sup>1</sup>Dexter et al. (2014)

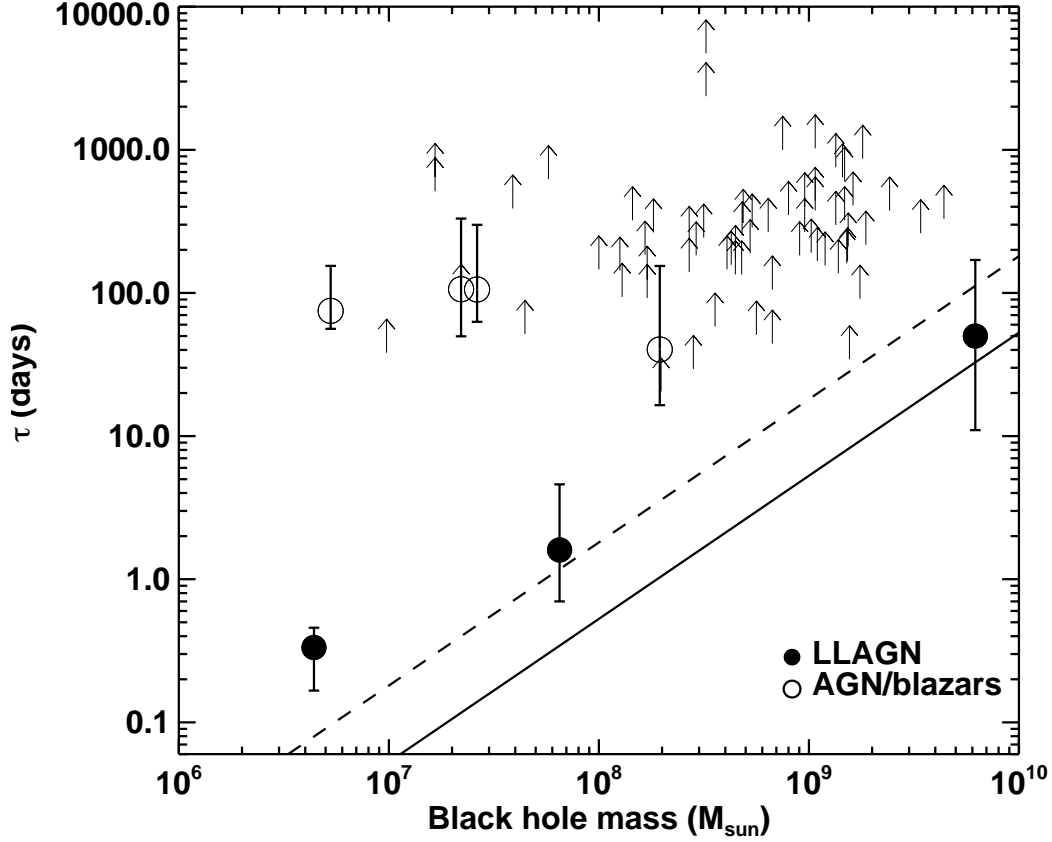


Fig. 4.— Black hole mass versus DRW time scale for the SMA calibrator source sample. LLAGN Sgr A\*, M81, and M87 are shown as filled in circles. Other AGNs from the SMA calibrator database with black hole masses are shown as open circles for detections and up arrows for lower limits on  $\tau$ . The time scales associated with AGN/blazars are significantly longer at the same black hole mass than those of the LLAGN. The inferred time scales for LLAGN variability increase with black hole mass, and are consistent with the predicted linear relationship from General Relativity. The solid line gives the period for the innermost stable circular orbit (ISCO); the dashed line gives the infall time for a disk with radius  $5R_S$ , a viscosity  $\alpha = 1$ , and a height  $H/R = 1$ .

best power-law fit is  $\tau \approx 0.3 \text{ day} (M_{\text{BH}}/4 \times 10^6 M_{\odot})^{0.7 \pm 0.1}$  (with a coefficient of determination  $R^2 = 0.996$ ). We consider the observed trend consistent with a linear relationship, however, given the small number of sources and the large uncertainties in  $\tau$  and  $M_{\text{BH}}$ . If the M87 mass were taken from gas dynamical measurements, for instance, then a linear law would be consistent with the data. The reliability of the correlation rests on only three LLAGN. This is a minimally small number of objects for a correlation, but these are the only LLAGN for which  $\tau$  can currently be determined. We are performing observational campaigns to increase the number of LLAGN with measured  $\tau$ .

A prediction of general relativity is that time scales around black holes should scale as  $\tau \sim R^{3/2} M_{\text{BH}}$ , where  $R$  is the radius in units of the event horizon size. This time scale reaches a minimum for a given  $M_{\text{BH}}$  when  $R$  is comparable to the size of the event horizon, and in that case one might expect to find a linear relationship between  $\tau$  and  $M_{\text{BH}}$ . This is clearly not borne out by the full sample: there is a large scatter in measured  $\tau$  values for regular AGN, and they do not fall on a linear track with the LLAGN. The discovery of such a relationship for the LLAGN suggests that we are measuring such minimum time scales from emission close to an event horizon.

This interpretation is consistent with our understanding of these sources inferred from their spectral energy distributions. For all three LLAGN, the spectra peak in the millimeter or submillimeter regime (Bower et al. 2015; Markoff et al. 2008; Doi et al. 2013). Synchrotron self-absorption leads to a large photosphere which shrinks until the spectral peak, where we can see down to the event horizon. At longer wavelengths, we expect longer timescales because of the larger scales of the photosphere. This larger photosphere is seen as a growing intrinsic image size with wavelength in VLBI observations of Sgr A\* (Bower et al. 2006) and M87 (e.g., Hada et al. 2011). The same effect shows up in the variability time scales for Sgr A\* and M81 and likely for M87. For Sgr A\*, Macquart & Bower (2006) found a characteristic time scale at wavelengths from 0.7 to 20 cm that ranged from 6 days to hundreds of days, increasing with wavelength. Additionally, we performed a DRW analysis of the 2cm M81 light curve (Ho et al. 1999) and found a lower limit to  $\tau$  of tens of days, much larger than the measured value at 1.3mm. In addition, for the case of Sgr A\*, the NIR variability time scale matches the submm value, consistent with the hypothesis of emission at both wavelengths emerging from the same region near the event horizon (Witzel et al. 2012). Thus, one should expect a similar relationship for other LLAGN with spectra peaking in the submm. The blazars and high power radio sources presumably do not follow a linear correlation because these sources are still optically thick at this wavelength. X-ray binaries in the low/hard state may also show the same correlation in the optically thin regime, although this may be difficult to observe due to the  $\lesssim 1$  sec time scales implied by the relationship and the rapidly evolving dynamics of these systems (Russell et al. 2014).

A similar relationship was found in the X-ray (McHardy et al. 2006) for black holes ranging from stellar to supermassive. This relationship, however, relied on a scaling factor based on the accretion rate, which we do not require here. This scaling factor could be interpreted as compensating between different values of  $R$  in the time scale corresponding to the X-ray emission region. In the LLAGN, we instead appear to have reached the minimum variability time scale corresponding to emission from event horizon scales around black holes.

The scaling relationship between black hole mass and variability time scale for LLAGN is an important insight for Event Horizon Telescope observations of these sources (Fish et al. 2013). These imaging observations will have resolutions as good as a few Schwarzschild radii and have the potential to probe fundamental gravitational physics (e.g., Lu et al. 2014; Broderick et al. 2014; Pen & Broderick 2014; Ricarte & Dexter 2015). The  $\tau - M_{BH}$  correlation shows that the compact sizes measured for these sources are actually colocated with the black hole. In addition, many of the fundamental parameters such as spin are degenerate with source physics parameters including the accretion rate, the jet inclination angle, the electron temperature distribution, the magnetic field strength and orientation, and the optical depth. Given the vastly different scales, environments, and physical properties of these three LLAGN systems, the existence of this correlation demonstrates a surprising coherence among these sources. These, and potentially other LLAGN with spectra peaking in the mm/submm can be treated as a unified class. Broadband spectra and light curve monitoring of other nearby LLAGN in the submm will add to the number of sources that fall into this class. Sources that do not follow this correlation, such as the majority of the SMA calibrators, may follow the relation at a higher frequency where the emission becomes optically thin.

The Submillimeter Array is a joint project between the Smithsonian Astrophysical Observatory and the Academia Sinica Institute of Astronomy and Astrophysics and is funded by the Smithsonian Institution and the Academia Sinica. This research has made use of the NASA/IPAC Extragalactic Database (NED), which is operated by the Jet Propulsion Laboratory, California Institute of Technology, under contract with the National Aeronautics and Space Administration.

## REFERENCES

- Blandford, R. D. & Konigl, A. 1979, *ApJ*, 232, 34
- Bower, G. A., Wilson, A. S., Heckman, T. M., Magorrian, J., Gebhardt, K., Richstone, D. O., Peterson, B. M., & Green, R. F. 2000, in *Bulletin of the American Astronomical*

- Society, Vol. 32, American Astronomical Society Meeting Abstracts, 1566
- Bower, G. C., Goss, W. M., Falcke, H., Backer, D. C., & Lithwick, Y. 2006, *ApJ*, 648, L127
- Bower, G. C., Markoff, S., Dexter, J., Gurwell, M. A., Moran, J. M., Brunthaler, A., Falcke, H., Fragile, P. C., Maitra, D., Marrone, D., Peck, A., Rushton, A., & Wright, M. C. H. 2015, *ApJ*, 802, 69
- Broderick, A. E., Johannsen, T., Loeb, A., & Psaltis, D. 2014, *ApJ*, 784, 7
- Cappellari, M., Neumayer, N., Reunanen, J., van der Werf, P. P., de Zeeuw, P. T., & Rix, H.-W. 2009, *MNRAS*, 394, 660
- Devereux, N., Ford, H., Tsvetanov, Z., & Jacoby, G. 2003, *AJ*, 125, 1226
- Dexter, J., Kelly, B., Bower, G. C., Marrone, D. P., Stone, J., & Plambeck, R. 2014, *MNRAS*, 442, 2797
- Doeleman, S. S., Fish, V. L., Schenck, D. E., Beaudoin, C., Blundell, R., Bower, G. C., Broderick, A. E., Chamberlin, R., Freund, R., Friberg, P., Gurwell, M. A., Ho, P. T. P., Honma, M., Inoue, M., Krichbaum, T. P., Lamb, J., Loeb, A., Lonsdale, C., Marrone, D. P., Moran, J. M., Oyama, T., Plambeck, R., Peimiani, R. A., Rogers, A. E. E., Smythe, D. L., Soohoo, J., Strittmatter, P., Tilanus, R. P. J., Titus, M., Weintraub, J., Wright, M., Young, K. H., & Ziurys, L. M. 2012a, *Science*, 338, 355
- Doeleman, S. S., Fish, V. L., Schenck, D. E., Beaudoin, C., Blundell, R., Bower, G. C., Broderick, A. E., Chamberlin, R., Freund, R., Friberg, P., Gurwell, M. A., Ho, P. T. P., Honma, M., Inoue, M., Krichbaum, T. P., Lamb, J., Loeb, A., Lonsdale, C., Marrone, D. P., Moran, J. M., Oyama, T., Plambeck, R., Primiani, R. A., Rogers, A. E. E., Smythe, D. L., Soohoo, J., Strittmatter, P., Tilanus, R. P. J., Titus, M., Weintraub, J., Wright, M., Young, K. H., & Ziurys, L. M. 2012b, *Science*, 338, 355
- Doeleman, S. S., Weintraub, J., Rogers, A. E. E., Plambeck, R., Freund, R., Tilanus, R. P. J., Friberg, P., Ziurys, L. M., Moran, J. M., Corey, B., Young, K. H., Smythe, D. L., Titus, M., Marrone, D. P., Cappallo, R. J., Bock, D., Bower, G. C., Chamberlin, R., Davis, G. R., Krichbaum, T. P., Lamb, J., Maness, H., Niell, A. E., Roy, A., Strittmatter, P., Werthimer, D., Whitney, A. R., & Woody, D. 2008, *Nature*, 455, 78
- Doi, A., Hada, K., Nagai, H., Kino, M., Honma, M., Akiyama, K., Oyama, T., & Kono, Y. 2013, in *European Physical Journal Web of Conferences*, Vol. 61, *European Physical Journal Web of Conferences*, 8008

- Emmanoulopoulos, D., McHardy, I. M., & Uttley, P. 2010, *MNRAS*, 404, 931
- Falcke, H. & Biermann, P. L. 1995, *A&A*, 293, 665
- Falcke, H., Körding, E., & Markoff, S. 2004, *A&A*, 414, 895
- Fish, V., Alef, W., Anderson, J., Asada, K., Baudry, A., Broderick, A., Carilli, C., Colomer, F., Conway, J., Dexter, J., Doeleman, S., Eatough, R., Falcke, H., Frey, S., Gabányi, K., Gálvan-Madrid, R., Gammie, C., Giroletti, M., Goddi, C., Gómez, J. L., Hada, K., Hecht, M., Honma, M., Humphreys, E., Impellizzeri, V., Johannsen, T., Jorstad, S., Kino, M., Körding, E., Kramer, M., Krichbaum, T., Kudryavtseva, N., Laing, R., Lazio, J., Loeb, A., Lu, R.-S., Maccarone, T., Marscher, A., Mart’i-Vidal, I., Martins, C., Matthews, L., Menten, K., Miller, J., Miller-Jones, J., Mirabel, F., Muller, S., Nagai, H., Nagar, N., Nakamura, M., Paragi, Z., Pradel, N., Psaltis, D., Ransom, S., Rodriguez, L., Rottmann, H., Rushton, A., Shen, Z.-Q., Smith, D., Stappers, B., Takahashi, R., Tarchi, A., Tilanus, R., Verbiest, J., Vlemmings, W., Walker, R. C., Wardle, J., Wiik, K., Zackrisson, E., & Zensus, J. A. 2013, *ArXiv e-prints*
- Gebhardt, K., Adams, J., Richstone, D., Lauer, T. R., Faber, S. M., Gültekin, K., Murphy, J., & Tremaine, S. 2011, *ApJ*, 729, 119
- Genzel, R., Eisenhauer, F., & Gillessen, S. 2010, *Reviews of Modern Physics*, 82, 3121
- Gurwell, M. A., Peck, A. B., Hostler, S. R., Darrah, M. R., & Katz, C. A. 2007, in *Astronomical Society of the Pacific Conference Series*, Vol. 375, *From Z-Machines to ALMA: (Sub)Millimeter Spectroscopy of Galaxies*, ed. A. J. Baker, J. Glenn, A. I. Harris, J. G. Mangum, & M. S. Yun, 234
- Hada, K., Doi, A., Kino, M., Nagai, H., Hagiwara, Y., & Kawaguchi, N. 2011, *Nature*, 477, 185
- Healey, S. E., Romani, R. W., Cotter, G., Michelson, P. F., Schlafly, E. F., Readhead, A. C. S., Giommi, P., Chaty, S., Grenier, I. A., & Weintraub, L. C. 2008, *ApJS*, 175, 97
- Healey, S. E., Romani, R. W., Taylor, G. B., Sadler, E. M., Ricci, R., Murphy, T., Ulvestad, J. S., & Winn, J. N. 2007, *ApJS*, 171, 61
- Ho, L. C. 1999, *ApJ*, 516, 672
- Ho, L. C., van Dyk, S. D., Pooley, G. G., Sramek, R. A., & Weiler, K. W. 1999, *AJ*, 118, 843

- Kasliwal, V. P., Vogeley, M. S., & Richards, G. T. 2015, *MNRAS*, 451, 4328
- Kelly, B. C. & Bechtold, J. 2007, *ApJS*, 168, 1
- Kelly, B. C., Bechtold, J., & Siemiginowska, A. 2009, *ApJ*, 698, 895
- Kormendy, J. & Ho, L. C. 2013, *ARA&A*, 51, 511
- Lu, R.-S., Broderick, A. E., Baron, F., Monnier, J. D., Fish, V. L., Doeleman, S. S., & Pankratius, V. 2014, *ApJ*, 788, 120
- MacLeod, C. L., Ivezić, Ž., Kochanek, C. S., Kozłowski, S., Kelly, B., Bullock, E., Kimball, A., Sesar, B., Westman, D., Brooks, K., Gibson, R., Becker, A. C., & de Vries, W. H. 2010, *ApJ*, 721, 1014
- Macquart, J.-P. & Bower, G. C. 2006, *ApJ*, 641, 302
- Markoff, S., Nowak, M., Young, A., Marshall, H. L., Canizares, C. R., Peck, A., Krips, M., Petitpas, G., Schödel, R., Bower, G. C., Chandra, P., Ray, A., Munro, M., Gallagher, S., Hornstein, S., & Cheung, C. C. 2008, *ApJ*, 681, 905
- McHardy, I. M., Koerding, E., Knigge, C., Uttley, P., & Fender, R. P. 2006, *Nature*, 444, 730
- Merloni, A., Heinz, S., & di Matteo, T. 2003, *MNRAS*, 345, 1057
- Pâris, I., Petitjean, P., Aubourg, É., Ross, N. P., Myers, A. D., Streblyanska, A., Bailey, S., Hall, P. B., Strauss, M. A., Anderson, S. F., Bizyaev, D., Borde, A., Brinkmann, J., Bovy, J., Brandt, W. N., Brewington, H., Brownstein, J. R., Cook, B. A., Ebelke, G., Fan, X., Filiz Ak, N., Finley, H., Font-Ribera, A., Ge, J., Hamann, F., Ho, S., Jiang, L., Kinemuchi, K., Malanushenko, E., Malanushenko, V., Marchante, M., McGreer, I. D., McMahon, R. G., Miralda-Escudé, J., Muna, D., Noterdaeme, P., Oravetz, D., Palanque-Delabrouille, N., Pan, K., Perez-Fournon, I., Pieri, M., Riffel, R., Schlegel, D. J., Schneider, D. P., Simmons, A., Viel, M., Weaver, B. A., Wood-Vasey, W. M., Yèche, C., & York, D. G. 2014, *A&A*, 563, A54
- Pen, U.-L. & Broderick, A. E. 2014, *MNRAS*, 445, 3370
- Plotkin, R. M., Markoff, S., Kelly, B. C., Körding, E., & Anderson, S. F. 2012, *MNRAS*, 419, 267
- Ricarte, A. & Dexter, J. 2015, *MNRAS*, 446, 1973

- Russell, T. D., Soria, R., Miller-Jones, J. C. A., Curran, P. A., Markoff, S., Russell, D. M., & Sivakoff, G. R. 2014, MNRAS, 439, 1390
- Schödel, R., Krips, M., Markoff, S., Neri, R., & Eckart, A. 2007, A&A, 463, 551
- Shen, J., Vanden Berk, D. E., Schneider, D. P., & Hall, P. B. 2008, AJ, 135, 928
- Shen, Y., Richards, G. T., Strauss, M. A., Hall, P. B., Schneider, D. P., Snedden, S., Bizyaev, D., Brewington, H., Malanushenko, V., Malanushenko, E., Oravetz, D., Pan, K., & Simmons, A. 2011, ApJS, 194, 45
- Strom, A. L., Siemiginowska, A., Gurwell, M. A., & Kelly, B. C. 2010, ArXiv e-prints
- Walsh, J. L., Barth, A. J., Ho, L. C., & Sarzi, M. 2013, ApJ, 770, 86
- Witzel, G., Eckart, A., Bremer, M., Zamaninasab, M., Shahzamanian, B., Valencia-S., M., Schödel, R., Karas, V., Lenzen, R., Marchili, N., Sabha, N., Garcia-Marin, M., Buchholz, R. M., Kunneriath, D., & Straubmeier, C. 2012, ApJS, 203, 18
- Woo, J.-H. & Urry, C. M. 2002, ApJ, 579, 530